Essential Readings in Light Metals: Aluminum Reduction Technology.
Edited by Geoff Bearne, Marc Dupuis and Gary Tarcy.

CRUSTING BEHAVIOR OF SMELTER ALUMINAS

Douglas W. Townsend and Larry G. Boxall

Martin Marietta Laboratories
Baltimore, Maryland 21227
USA

The mechanism of cell crust formation has been investigated by studying petrographic thin sections of crusts made from different ores. Crusts form when cryolite bath soaks into alumina ore, selectively dissolving and cementing it together. Crusts were made by adding both reacted and unreacted commercial ores to a typical smelter bath. Crusting behavior was correlated with ore type, size fraction, and whether or not the ore was previously reacted with bath fume in a dry scrubber. Reacted ores are wetted faster and form softer crust. Petrographic thin sections of crusts show cemented-together alumina particles that are relatively unattacked by penetrating bath. Crust is formed because γ-alumina dissolves faster in the bath and has a higher solubility limit than α-alumina, causing local supersaturation. γ-alumina continues to dissolve, whereas α-alumina crystallizes to cement ore into crust.

Introduction

Smelter alumina ores with similar physical properties often display very different crusting behavior on reduction cells. In recent years, various aluminum companies have been trading ore so that individual smelters often receive consecutive shipments from different Bayer alumina plants. This practice often results in reduction plant upsets involving cell mucking, escape of excessive amounts of bath fume and difficulty in breaking or maintaining crust.

On a side-break Soderberg cell, an alumina ore that has a relatively low crusting tendency is desirable because it forms a soft crust on a cool area of the cell where there is little agitation. This crust should be easily pushed into the bath by breaker bars and also form quickly before the bath soaks completely through new ore, to prevent loss of fume and heat. Center-break cells and point-fed cells require alumina ore with a relatively high crusting tendency to resist collapsing into the bath in relatively hot and well agitated areas of the cell.

Alumina ores used in western countries generally can be classified as having a sandy texture. Typically 95-98% of the alumina particles will pass a 100-mesh screen, whereas the amount of -325 mesh may vary from less than 10% to more than 35%. The α-alumina content typically ranges from 10% to 30%. Most alumina ore particles are composed of intimate mixtures of both cubic γ-alumina and hexagonal α-alumina crystals as can be seen using an optical microscope and an oil having an index of refraction between that of γ-and α-alumina.

From studies of dissolution rates of individual alumina particles in cryolite bath, Thonstad (1) showed that γ-alumina dissolves faster than α-alumina. The same result was obtained by Gerlack et al. (2) using rotating disks. Although it has been recognized that sandy aluminas tend to form hard crusts, the mechanism of cementing undissolved alumina particles together to form crust has been attributed to networks of α-alumina crystals (3,4,5). These are always found in superficial examinations of the surfaces of ore crusts after cryolite has been leached. The actual cementing together of alumina particles, however, has not been illustrated nor has the process of cementing been described. In this paper, we will further examine the mechanism of crusting of alumina ores.

Alumina Ore Properties

Four alumina ores from different Bayer plants were selected for this study. They can all be classified as sandy aluminas, although they differ from each other considerably in physical appearance. The physical properties of the virgin ores is given in Table I and of reacted ores in Table II. The amounts of chemicals absorbed from the cell fume to make reacted ores in the dry scrubbers are given in Table III.

The physical appearance of the four virgin alumina ores, as viewed by scanning electron microscope (SEM), are shown in Figure 1. Each ore has physical properties typical of sandy alumina, including size distribution, low α-alumina content, high surface area and low angle of repose.

TABLE I. Physical Properties of Virgin Aluminas

Alumina Mesh	A (wt.%)	B (wt.%)	C (wt.%)	D (wt.%)
+100	0.4	5.8	1.2	1.4
100-200	46.5	50.8	53.6	58.8
200-325	36.5	23.3	34.6	29.8
-325	16.6	20.1	10.6	10.0
Sub-screen of -325 mesh diameter μm				
50.8-40.3	22.5	10.8	16.0	15.5
40.3-32.0	42.6	12.0	17.3	23.2
32.0-25.4	22.2	10.4	12.3	16.1
25.4-20.2	7.9	7.7	8.6	11.3
20.2-16.0	2.5	7.5	7.3	9.2
16.0-12.7	1.1	7.8	6.7	7.0
12.7-10.08	0.4	8.3	6.0	5.1
10.08-8.00	0.4	7.7	4.9	3.6
8.00-6.35	0.0	8.6	5.2	3.2
6.35-5.04	0.0	7.1	4.5	2.4
5.04-4.00	0.0	5.0	4.1	1.5
4.00-3.17	0.0	2.9	2.6	0.8
3.17-2.52	0.0	1.4	1.7	0.4
2.52-2.00	0.0	1.2	1.5	0.3
< 2.00	0.0	1.4	1.0	0.3
Specific surface area m^2/g				
+325	67.0	41.2	68.4	65.5
-325	55.6	31.8	38.2	29.7
All fractions	65.1	39.4	65.2	61.9
% α-alumina	20.8	14.7	19.6	20.2
Angle of repose, degrees	28.3	26.8	30.8	29.3
Bulk density (g/cm^3) tamped	1.16	1.25	1.06	1.09
Untamped	1.01	1.06	0.91	0.98

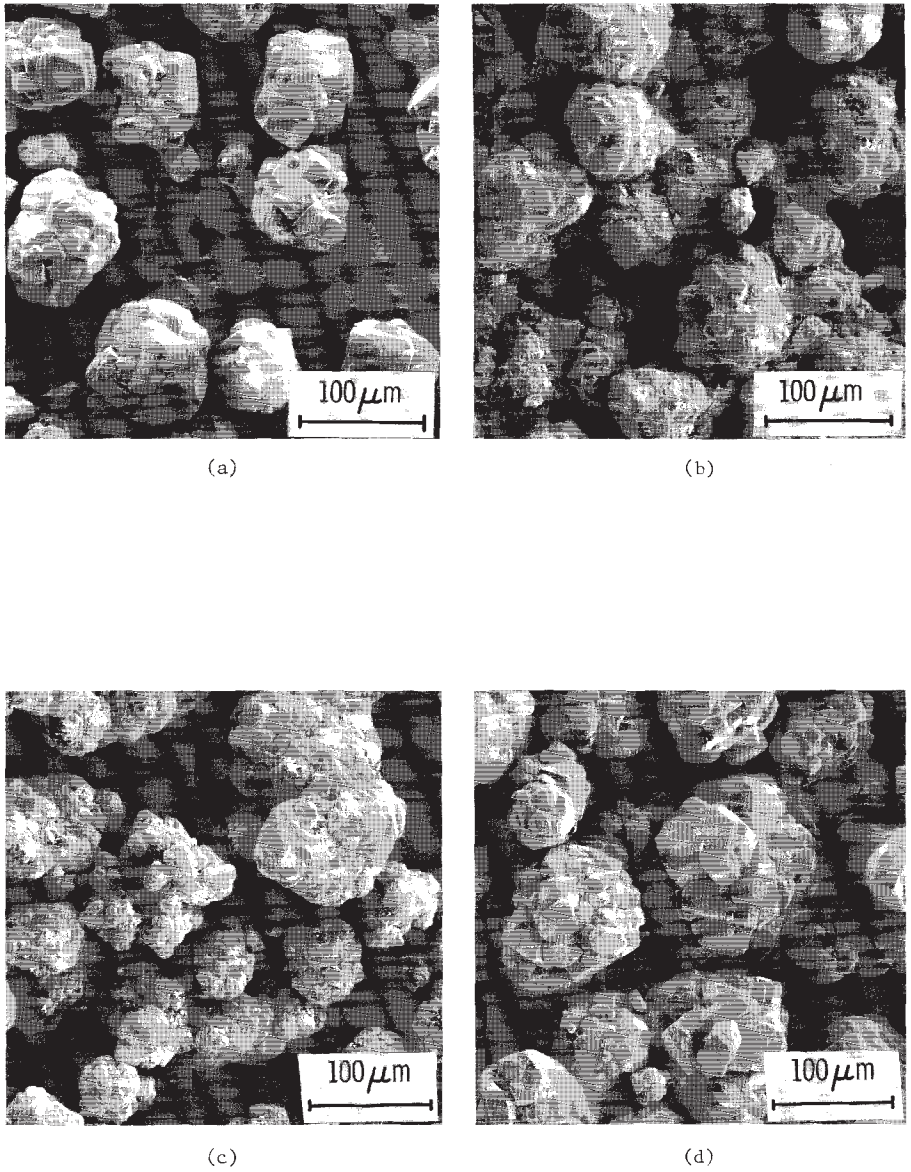

(a) (b)

(c) (d)

Figure 1. Scanning electron micrographs of virgin aluminas: (a) alumina A, (b) alumina B, (c) alumina C, and (d) alumina D.

TABLE II. Physical Properties of Reacted Aluminas

Alumina Mesh	A (wt.%)	B (wt.%)	C (wt.%)	D (wt.%)
+100	0.2	5.9	3.3	0.8
100-200	39.8	57.6	55.4	75.7
200-325	49.5	22.9	36.1	21.8
-325	10.5	13.6	5.2	1.7
Sub-screen of -325 mesh diameter μm				
50.8-40.3	48.8	6.1	17.9	41.5
40.3-32.0	27.5	8.2	24.4	25.5
32.0-25.4	9.0	7.4	13.9	10.8
25.4-20.2	3.6	6.1	8.2	5.5
20.2-16.0	2.0	6.4	6.3	3.8
16.0-12.7	1.5	8.0	5.5	3.1
12.7-10.08	1.3	8.8	4.9	2.6
10.08-8.00	1.4	9.0	4.0	2.0
8.00-6.35	1.2	11.0	4.3	1.7
6.35-5.04	1.1	10.0	3.7	1.4
5.04-4.00	0.9	7.9	2.0	0.8
4.00-3.17	0.6	4.8	1.8	0.4
3.17-2.52	0.3	2.4	0.9	0.1
2.52-2.00	0.3	2.0	0.7	0.2
< 2.00	0.3	1.6	0.6	0.2
Specific surface area m^2/g				
+325 mesh	58.4	37.5	53.2	59.0
-325 mesh	37.6	27.6	33.1	32.4
All fractions	56.2	36.4	52.2	58.4

Experimental

Alumina crusts were made in the laboratory by adding 2-, 4-, and 8-g samples of commercial ores to the surface of a cryolite bath held at 985°C. The basic bath composition was CaF_2 - 3.5%, AlF_3 - 7.5%, and Na_3AlF_6 - 89%. The bath ratio was 1.25. During the course of the experiments, the dissolved Al_2O_3 in the bath ranged from 2% through saturation. About 1600 g of bath was held in a graphite crucible, 8 cm in diameter by 19 cm tall, contained in an Inconel pot. Control thermocouples were kept outside the Inconel pot near the furnace windings. The bath temperature, measured by a thermocouple just above the bath surface, differed by less than 5°C from temperatures measured throughout the bath. There was no tendency to form crust by bath freezing. The top of the furnace was covered with Marinite®; argon flowed over the bath surface between experiments.

TABLE III. Fluoride, Carbon and Sulfur Analyses of Alumina Ores

Alumina	Fluoride (wt.%)	Carbon (wt %)	Sulfur (wt.%)
A Virgin	0.030	---	0.001
A Reacted	0.76	1.27	0.28
B Virgin	0.030	---	0.025
B Reacted	1.07	1.62	0.21
C Virgin	0.005	---	0.010
C Reacted	1.60	0.93	0.21
D Virgin	0.040	---	0.012
D Reacted	1.14	1,99	0.25

A batch of bath salts was warmed to 500°C overnight, melted at 1030°C, and cooled to 985°C, which was from 5-35°C above the melting point of the bath. The minimum freezing point of this bath is 948°C at 8% dissolved Al_2O_3. Crusting tests were made by dropping 2-g samples of unheated alumina from a 1/2-inch tube having a spring-loaded cone stopper from a distance of 5 cm.

Four-gram samples of alumina ore and bath were recovered 10 seconds after wetting for examination of bath penetration before a crust could develop. Crust produced from 8-g samples of alumina ore were recovered three minutes after wetting for studies of the crust-forming process and recrystallization of alumina.

Results

The time for bath to wet the alumina, the nature of the crust, and the times for the alumina to sink and finally to dissolve into both stagnant and stirred bath were observed and recorded in Table IV.

The crust produced by each of the virgin alumina ores, either fell quickly to the crucible bottom in one to four large chunks or broke up into flakes and slowly sank. The following definitions have been used in Table IV to describe the crusting tendency and dissolution behaviors of the ores.

TABLE IV. Alumina Dissolution Properties

Sample Identification	Experiment	Wetting Time (seconds)	Sinking Time (seconds)	Time to Complete Dissolution (seconds)	Crusting and Dissolution Behavior[1]
A Virgin	Unstirred	8	63	375	1a
A Reacted	"	9	FLT[2]	354	2c
B Virgin	"	11	129	237	1b
B Reacted	"	6	FLT	300	2c
C Virgin	"	5	90	283	1b
C Reacted	"	5	FLT	408	2c
D Virgin	"	6	120	353	1b
D Reacted	"	5	FLT	424	2c
A Virgin	Stirred 250 rpm	5	22	161	1a
A Reacted	"	3	10	100	2b
B Virgin	"	5	25	44	2b
B Reacted	"	3	30	49	2c
C Virgin	"	3	9	113	1b
C Reacted	"	5	20	129	2c
D Virgin	"	3	11	126	1c
D Reacted	"	5	15	82	2c
A Virgin -325	Unstirred	4	38	248	1a
A Virgin +325	"	2	200	298	1a
A Reacted -325	"	30	FLT	150	2b
A Reacted +325	"	6	270	504	1b
B Virgin -325	"	4	60	756	2c
B Virgin +325	"	7	90	268	1a
B Reacted -325	"	33	90	536	2b
B Reacted +325	"	3	56	140	2c
C Virgin -325	"	9.5	17	594	2a
C Virgin +325	"	9.5	24	606	1a
C Reacted -325	"	6	139	179	2c
C Reacted +325	"	4	FLT	645	2c
D Virgin -325	"	6	75	402	1a
D Virgin +325	"	5	140	453	1a
D Reacted -325	"	15	FLT	75	2c
D Reacted +325	"	2	FLT	345	2c

1 See text for explanation
2 The aluminum did not sink in the bath; it floated on the bath surface until dissolved

TABLE IV cont'd

Sample Identification	Experiment	Wetting Time (seconds)	Sinking Time (seconds)	Time to Complete Dissolution (seconds)	Crusting and Dissolution Behavior
A Virgin -325	Stirred 225 rpm	9	14	150	1a
A Virgin +325	"	4	13	252	1a
A Reacted -325	"	6	FLT	192	2c
A Reacted +325	"	4	71	120	2b
B Virgin +325	"	4	52	91	2b
B Virgin -325	"	4	14	64	1b
B Reacted +325	"	12	FLT	287	2c
B Reacted -325	"	4	36	97	2c
C Virgin -325	"	3	15	162	1b
C Virgin +325	"	3	35	148	1a
C Reacted -325	"	11	36	155	2c
C Reacted +325	"	3	54	175	1b
D Virgin -325	"	7	20	123	1a
D Virgin +325	"	6	20	244	1a
D Reacted -325	"	3	54	181	2c
D Reacted +325	"	4	41	148	2c

Crusting Tendency

1. Forms a coherent hard crust with mechanical strength, like a white ice
2. Forms a soft crust without mechanical strength, like wet snow,

Dissolution Behavior

a. The crust sank to the bottom of the crucible in one or several large broken pieces and slowly melted away

b. The crust broke up on the surface and sank in a large number of small pieces or flakes, many of which dissolved while sinking

c. The crust largely dissolved away while floating on the surface of the bath with only a few flakes breaking away.

Alumina ore A produced by far the hardest crust, i.e., like a white ice, whereas alumina ore B produced the softest crust, i.e., like a wet snow. Ores C and D produced crusts softer than ores A but harder than B. Compared to virgin ores, reacted ores produce a relatively soft crust due to desorbing gasses. The crust tends to float on the bath because of trapped gas bubbles and carbon particles. Wetting, sinking and dissolving

were each accelerated by stirring; however, the basic character of each ore and crust was essentially unchanged.

When each of the ores was divided into a coarse fraction (+325 mesh) and a fine fraction, some changes in crusting behavior were observed. In general, the coarser fraction wetted faster and tended to produce a harder crust than did the fine fraction.

Leaching Tests on Crusts

Crust hardness can be tested by boiling pieces of frozen crust in 3.3% aluminum chloride solution for 10 minutes to remove the cryolite bath. This procedure is derived from a gravimetric analysis of dissolved alumina in cryolite bath. Cryolite bath is completely leached away from the alumina ore and α-alumina platelets.

Crust made from ores A and C remained intact after the bath was leached out, whereas crusts made from ores B and D disintegrated into powder. The soft crusts made from ores B and D apparently contained no extensive large-range network of cemented-together alumina ore particles.

Crust Formation Analysis

Ore crust forms when undissolved alumina particles cement-together into a strong three-dimensional network. When ore is first placed on bath, some freezing occurs as the ore is warmed and alumina dissolves, saturating the intruding bath. To heat alumina ore to bath temperature requires 27.5 kcal/mole for γ-alumina and 26.2 kcal/mole for α-alumina (6). We determined from analysis of photographs of thin sections (Figure 2) that alumina ores A and B each soak up about 35% by volume bath. Saturating this intruded bath with dissolved alumina only requires from 0.3 to 0.6 kcal/mole of ore (7). The heat required from the cell to form crust is essentially only that necessary to heat the ore to the bath temperature. Dissolution and radiation from the surface of the crust causes the crust to remain a few degrees cooler than the bath.

Optical photographs of petrographic thin sections prepared from cryolite-wetted alumina ores A and B along with intruded bath are seen in Figure 2. Conversion of the wetted alumina ores to crust from continued exposure to the bath (3 minutes) are shown in Figure 3. Ore A shows a high degree of particle-to-particle contact in both the wetted ore and hard crust, whereas ore B shows relatively less. Many of the alumina particles actually appear to be free floating in the soft crust. A high degree of continuous physical contact between particles of undissolved alumina is required to form a hard crust. Any process, including agitation, desorption of gas from reacted ore, and additional bath intruding into wetted ore B, clearly disrupts the crust-forming process. During the short time available for crust forming, 12% additional bath intruded the wetted ore and dispersed the ore particles so they did not grow together to form a hard crust. The bath occupies ∿ 47% of the volume of the soft crust, whereas only ∿ 39% of the volume is occupied by the bath in the hard crust.

Samples of crust that have been air cooled and leached appear to be composed of undissolved alumina ore particles covered by α-alumina platelets, 0.5-μm in diameter, Figures 4 and 5. These thin platelets merely occupy the space filled with the intruded bath. There is no apparent difference in the appearance of these thin platelets that cover the exposed surface of the

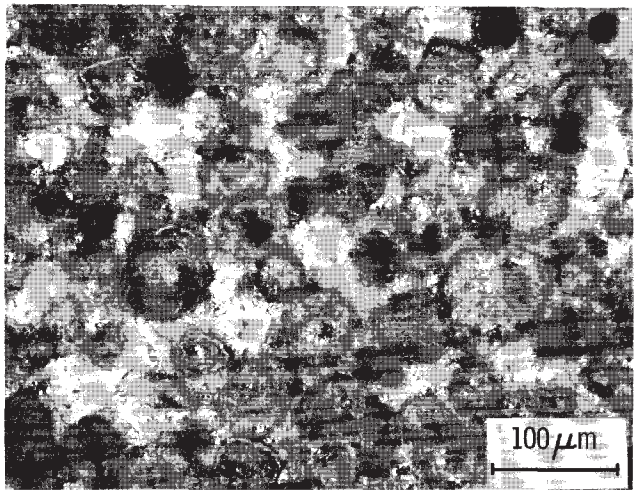

(a)

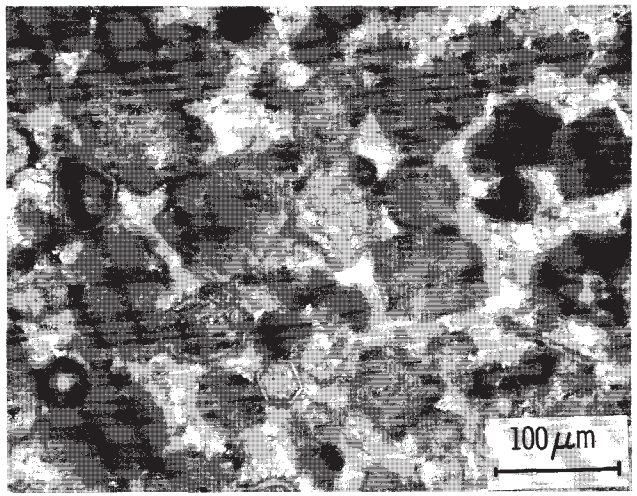

(b)

Figure 2. Petrographic thin sections of wetted cryolite ores: (a) alumina A and (b) alumina B.

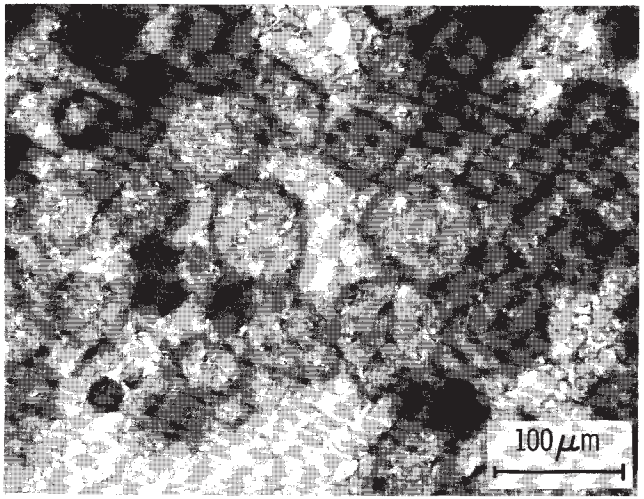

(a)

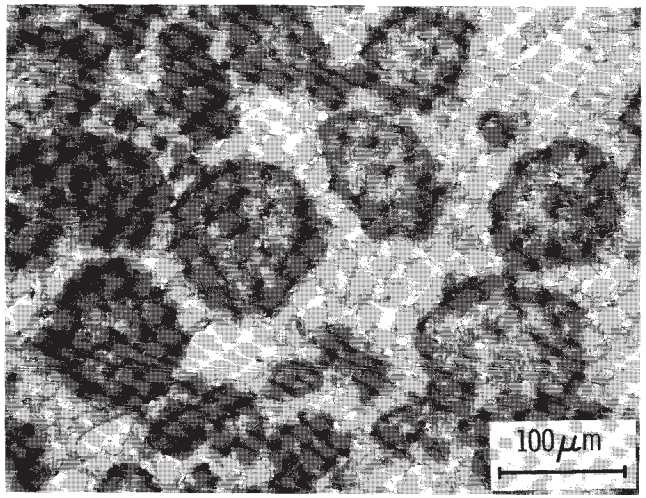

(b)

Figure 3. Petrographic thin sections of crusts: (a) alumina A and (b) alumina B after three minute of wetting by cryolite.

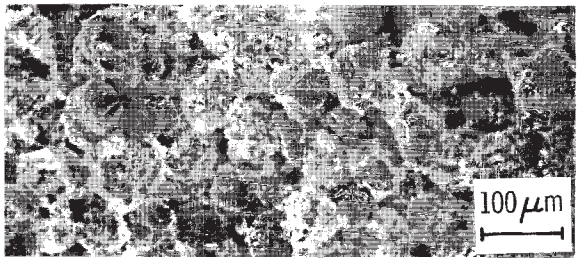

Figure 4. Scanning electron micrograph of leached crust, alumina ore A.

alumina ore particles from hard and soft crust. They merely froze out of the alumina-saturated bath during air cooling and did not contribute to crusting. If these thin α-alumina platelets had formed the crust cement, both crusts should have been equally hard.

It has been postulated by Less (3) that α-alumina platelets constitute the cement that produces ore crusts made from sandy alumina. The rapid growth of α-alumina to cross link or fuse together adjacent grains of alumina ore to form crust has been described by Johnston and Richards (5). The thin platelets shown in Figures 4 and 5, however, are not the ones that cement-together the ore to form crust. The cementing α-alumina platelets can be seen only in Figure 6 where sections have been cut through the crust, happening to intercept the points of contact between alumina ore particles. The crust cement is in fact composed of α-alumina platelets, but each is about three times as thick as the platelets that freeze out of the bath. As seen in an edge view, each of these crust-forming α-alumina platelets in Figure 6 is about 1.5-μm thick. Masses of them form a tight envelope of tangential and radial crystals surrounding the alumina ore particles in a layer about 5-μm thick. These thick crystals in hard crust almost completely fill the space between adjacent alumina ore particles. The difference in thickness between the cementing α-aluminum crystals and those that merely froze when the sample was quickly cooled can be seen in Figure 6.

X-ray analysis of samples of crust taken from bath three minutes after wetting shows that a considerable amount of the γ-alumina originally present in the alumina ore has recrystallized to α-alumina. Alumina, recovered from hard crust made from ore A, was 68% α-alumina compared with only 20.8% in the virgin ore. The soft crust made from ore B had converted from 14.7% to 93% α-alumina during three minutes of exposure to the bath. This shows that the fluoride "mineralizer" in the bath does in fact greatly accelerate recrystallization of the ore during the crust-forming process. The conversion of γ-alumina to α-alumina is thermodynamically favored with a Gibbs free energy of 0.78 kcal/mole (6). In the absence of the fluorides, at 985°C, 10 to 14 hours is required to get these degrees of conversion of γ-alumina to α-alumina (7). The rates of conversion to α-alumina of the ore particles in cryolite bath is rapid but crust forming is an even faster process. It is most significant that γ-alumina can be found in hard crust, because a thermodynamic analysis predicts that γ-alumina should be slightly more soluble in cryolite bath than α-alumina.

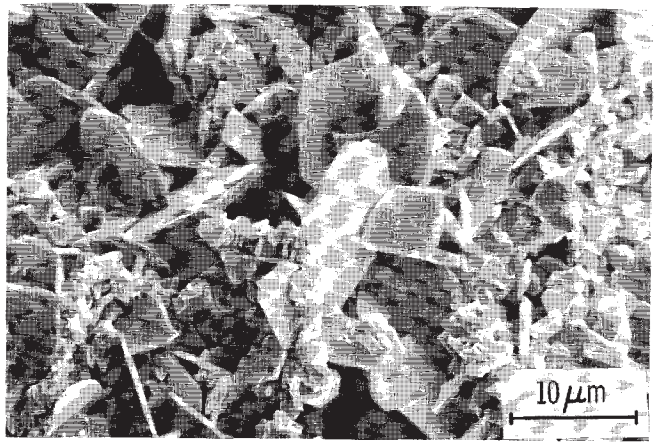

(a)

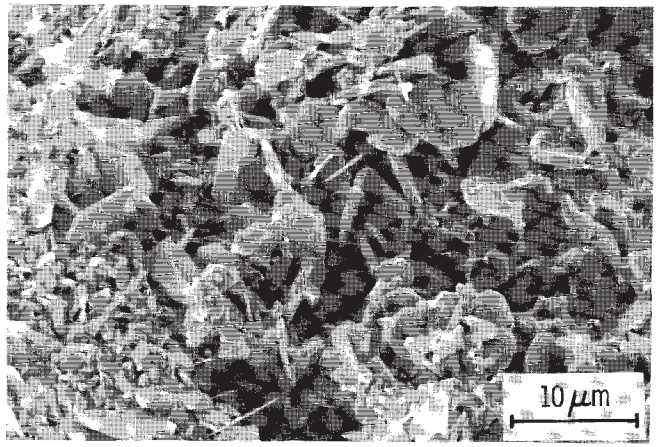

(b)

Figure 5. Scanning electron micrograph of leached crusts after three minutes of wetting by cryolite: (a) hard crust, alumina ore A; and (b) soft crust, alumina ore B.

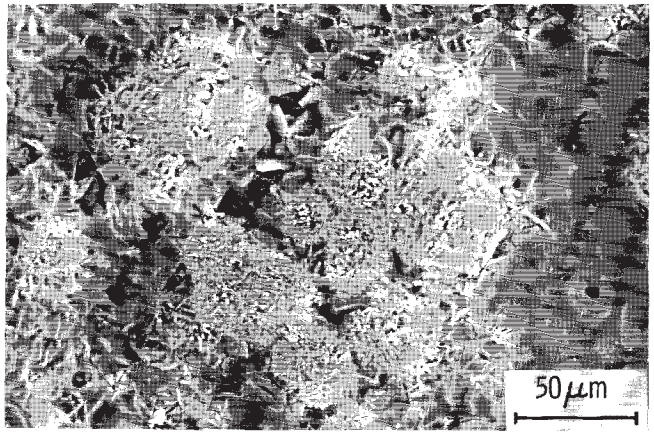

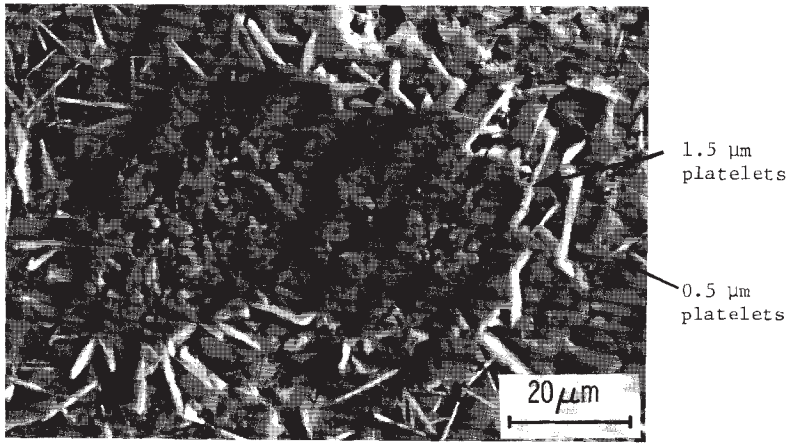

Figure 6. Scanning electron micrographs of cross sections of hard crust after three minutes of wetting by cryolite, alumina ore A.

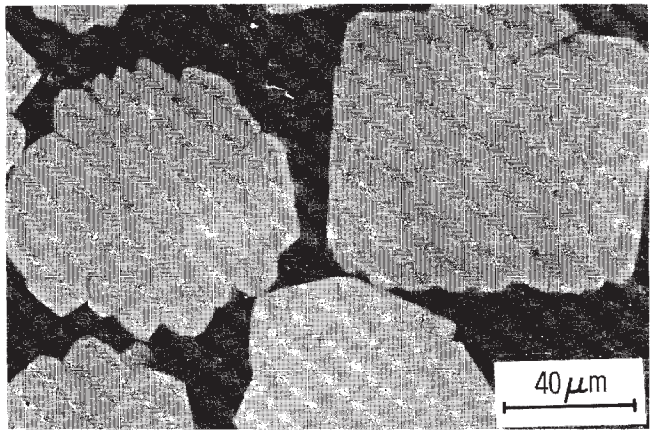

Figure 7. Scanning electron micrograph of cross section of virgin alumina ore A.

Figure 7 shows a cross section of alumina of ore A, which by X-ray analysis contained only 18% α-alumina. The 82% γ-alumina (by difference) has a homogeneous, nearly amorphous structure derived from calcination of aluminum trihydrate crystals (Gibbsite), precipitated in a Bayer plant from sodium hydroxide solutions supersaturated with sodium aluminate. After only three minutes exposure to the bath, the cores of these particles display the characteristic appearance of floury α-alumina of the type usually used in Europe, Figure 6. According to X-ray analysis, the ore has been converted to 68% α-alumina. By difference, the alumina particles taken from the crust still contained 32% γ-alumina so we may conclude that the crust-forming process was continuing when the sample was taken from the bath. This ore forms a very hard crust that simply sinks to the bottom of the crucible in one or a few large chunks and then dissolves into the bath from exposed surfaces without breaking apart.

In contrast, the soft crust formed from ore B contained only 9% γ-alumina after 3 minutes, showing that the crust-forming process was almost completed. Crust made from this ore tends to break up into small flakes and dissolve easily into the bath. This crust is easily broken by stirring. Previous observations (3) that floury high α-alumina has very poor crusting behavior are consistent with our proposed crusting mechanism.

Thus, the most likely mechanism for ore crust formation is the dissolution of γ-alumina into the bath and the simultaneous growth of α-alumina crystals on the same or adjacent particles of alumina ore. It takes several moments for the strong, thick α-alumina platelets to form. The intruded bath transports dissolved alumina by diffusion from less thermodynamically stable alumina particles in the crust. Diffusion distances between dissolving and growing crystals in crusts are very short and the intruded bath quickly becomes slightly supersaturated with respect to α-alumina. The crust-forming process continues for several minutes until the γ-alumina is depleted by dissolution or direct recrystallization within undissolved particles of alumina ore to α-alumina.

Conclusions

We are in general agreement with previously proposed mechanisms for alumina ore crusting. The formation of strong ore crusts does require strong α-alumina platelets to cement-together particles of undissolved ore. Crusting occurs because γ-alumina dissolves and supersaturates the intruded bath, thereby causing the growth of α-alumina platelets between undissolved alumina ore particles. The crusting process must occur within a few minutes because the bath fluorides simultaneously catalyze the recrystallization of undissolved γ-alumina to α-alumina which is a poor crust former. A high degree of particle-to-particle contact in the alumina ore is required for several moments after the aluminum ore is wetted by bath for a strong crust to form. It is still necessary to perform crusting tests to determine the types and relative strengths of crusts formed from different ores. Crust-forming tendencies cannot be correlated with easily measurable physical properties such as relative amounts of γ-alumina and particle size. In general, crust-forming tendencies are reduced by reacting the ore with bath fume in a dry scrubber and by the presence of a high fraction of -325 mesh fines.

Laboratory alumina-crusting tests and optical examination of petrographic thin sections of the formed crusts provide a means to screen ores for their potential impact on established smelter operations. The petrographic thin cross-section photographs provide crust-forming data normally obscured by the alumina-containing bath and can be used to evaluate potential new alumina sources for aluminum smelters.

Acknowledgement

The authors wish to thank Martin Marietta Alumina for permission to publish this work and the acknowledge laboratory assistance of W. Montague of Martin Marietta Laboratories.

References

1. J. Thonstad, F. Nordmo, and J.B. Paulsen, "Dissolution of Alumina in Molten Cryolite," Light Metals, (1971) pp. 213-222.

2. J. Gerlack, U. Hennig, and K. Kern, "The Dissolution of Aluminum Oxide in Cryolite Melts," Light Metals, 1 (1974) pp. 49-61.

3. L.N. Less, "The Crusting Behavior of Smelter Aluminas," Metallurgical Transactions, B, 8B, (1977) pp. 219-225.

4. A.R. Johnson, "Alumina Crusting and Dissolution in Molten Electrolyte," Journal of Metals, 34 (3) (1982) pp. 63-68.

5. T.J. Johnston and N.E. Richards, "Correlation Between Alumina Properties and Crusts," Light Metals, 1 (1983) pp. 623-639.

6. D.R. Stull and H. Prophet, JANAF Thermodynamic Tables, United States Department of Commerce (1971).

7. C.J.P. Steiner, D.P.H. Hasselman, and R.M. Spriggs, "Kinetics of the Gamma-to-Alpha Alumina Phase Transformation," Journal of the American Ceramic Society, 54 (8) (1971) pp. 412-413.

8. O.A. Asbjϕrnsen and J.A. Andersen, "Kinetics and Transport Processes in the Dissolution of Aluminum in Cryolite Melts," Light Metals 1 (1977) pp. 137-152.